Available online at www.sciencedirect.com
ScienceDirect
Journal of Photochemistry and Photobiology A: Chemistry 189 (2007) 128–134
Journal of Photochemistry and Photobiology A:Chemistry
www.elsevier.com/locate/jphotochem

UV-A induced photochemical formation of *N*-nitrosodimethylamine (NDMA) in the presence of nitrite and dimethylamine

Changha Lee, Jeyong Yoon *

School of Chemical Engineering, College of Engineering, Seoul National University, San 56-1, Sillim-Dong, Gwanak-Gu, Seoul 151-742, Republic of Korea

Received 17 October 2006; received in revised form 28 December 2006; accepted 17 January 2007
Available online 21 January 2007

Abstract

The photochemical nitrosation of dimethylamine (DMA) has been suggested as a possible pathway for the occurrence of *N*-nitrosodimethylamine (NDMA) in aquatic environments. The aim of this study was to investigate the formation of NDMA from the nitrosation of DMA during nitrite (NO_2^-) photolysis in aqueous solution by varying several of the experimental parameters. NDMA was formed at neutral pH, in the presence of DMA and NO_2^- under UV-A irradiation, and exhibited an increase in concentration with irradiation time. Increasing the concentrations of DMA and NO_2^- led to enhanced NDMA formation. Through experiments employing $^\bullet$OH scavenger (*t*-BuOH), $^\bullet$OH was found to play an important role in the production of nitrosating agents during the photolysis of NO_2^-. The optimum pH for the formation of NDMA was around 10. This pH dependence was explained by the dual role of deprotonated DMA as a nucleophile, which enhances the nitrosation reaction between nitrosating agents and DMA, and a hydroxyl radical ($^\bullet$OH) scavenger, which reduces the production of nitrosating agents. A higher concentration of NDMA was obtained under N_2 condition due to the lower quantum yield for NDMA photolysis in the absence of oxygen. Various anions, including phosphate ions in the buffer solution, retarded the formation of NDMA, possibly due to degradation of the nitrosating agents.
© 2007 Elsevier B.V. All rights reserved.

Keywords: *N*-Nitrosodimethylamine (NDMA); Dimethylamine; Nitrite; Photolysis; Ultraviolet (UV) irradiation

1. Introduction

N-Nitrosamines have been known as mutagenic, carcinogenic and teratogenic compounds since the 1960s. In recent years, *N*-nitrosodimethylamine (NDMA) has been recognized as an emerging contaminant in drinking water and wastewater [1,2], as trace levels have been detected, with the help of the advanced analytical technologies, in surface and drinking waters in North America. The US EPA classifies NDMA as a probable human carcinogen, with a 10^{-6} cancer risk level of 0.7 ng/L. The California Department of Health Services and the Ontario Ministry of the Environment have established interim drinking water levels for NDMA at 10 and 9 ng/L, respectively.

A number of studies have attempted to elucidate the mechanisms of NDMA formation in water. Recently, several research groups found that NDMA can be formed as a disinfection byproduct from chloramination [3,4]. According to one study, chloramination of secondary wastewater and surface water was found to form 100 and 10 ng/L NDMA, respectively [5]. The mechanism responsible for the formation of NDMA by chloramination has been suggested to involve the formation of 1,1-dimethylhydrazine (unsymmetrical dimethylhydrazine, UDMH) by the reaction of dimethylamine (DMA) with monochloramine, with the subsequent oxidation to NDMA [3,4].

Another pathway for the formation of NDMA in aqueous solution is the reaction of DMA with nitrous acid (HNO_2), which is traditionally the best known mechanism for the nitrosation of DMA [6]. Nitrous acid (HNO_2) in aqueous acidic solution (pH < 5) is known to form nitrosating agents of the type $NO^{\delta+}$–$Y^{\delta-}$, which is a complex of the nitrosonium ion (NO^+) with stable anions. These nitrosating agents transfer the NO^+ entity to DMA through nucleophilic (S_N2) displacement to yield NDMA, as described in reaction (1). The formation of NDMA from the reaction of DMA with HNO_2 is known to have an optimum around pH 3.

(1)

* Corresponding author. Tel.: +82 2 880 8927; fax: +82 2 876 8911.
E-mail address: jeyong@snu.ac.kr (J. Yoon).

1010-6030/$ – see front matter © 2007 Elsevier B.V. All rights reserved.
doi:10.1016/j.jphotochem.2007.01.022

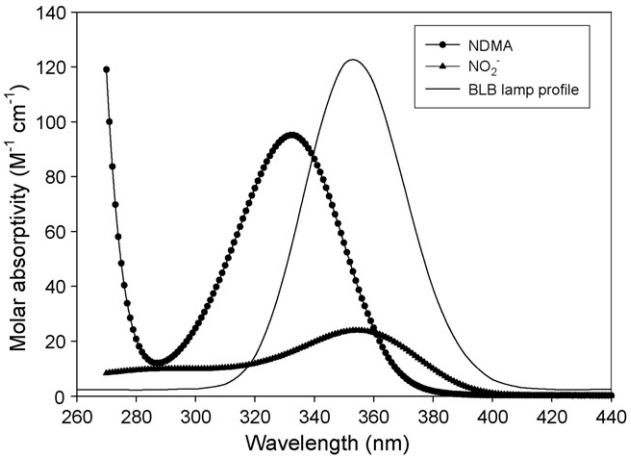

Fig. 1. Molar absorption coefficients of NDMA and nitrite, and the BLB lamp profile as a function of the wavelength.

In neutral or alkaline aqueous solutions, the reaction of DMA with HNO_2 produces insignificant amounts of NDMA, as no nitrosating agents can be formed from the nitrite ion (NO_2^-) (pK_a of $HNO_2 = 3.37$). However, UV irradiation on NO_2^- solution can produce nitrosating agents. The photolysis of NO_2^- is known to produce various nitric oxide species, of which N_2O_3 and N_2O_4 can act as nitrosating agents [7]. Significant photochemical nitrosation of DMA by the nitrosating agents produced from the photolysis of NO_2^- due to sunlight can occur in natural aquatic environments, since NO_2^- absorbs light at wavelengths up to 400 nm (Fig. 1).

One previous study has experimentally shown that NDMA can be photochemically formed from DMA during the photolysis of NO_2^- under light irradiation from both medium-pressure Hg lamp with a Pyrex UV cut-off filter ($\lambda > 300$ nm) and sunlight [8], with yields up to 35%, depending on UV irradiation time, concentration of NO_2^- and solution pH. This observation suggests that the photolysis of NO_2^- can be a major source of NDMA formation in aquatic environments, when considering the yield of NDMA from chloramination is only <3% [3,4]. However, the high yield of NDMA by the photolysis of NO_2^- needs to be reexamined, since NDMA is known to be highly photolabile, with quantum yields around 0.31 [9,10], which are much higher than those of NO_2^-; e.g. 0.046 at 351 nm [7]. Significant NDMA photolysis can occur simultaneously with its formation. Moreover, the study only provided limited information on the influences of water parameters on the formation of NDMA.

In the present work, attempts were made to reinvestigate the photochemical formation of NDMA from DMA in the presence of NO_2^-. Various parameters, such as the concentrations of DMA and NO_2^-, solution pH, dissolved oxygen and the presence of a hydroxyl radical ($^{\bullet}OH$) scavenger or (in)organic anions were tested, with the results discussed in relation to the reactions of radical species and nitrosating agents produced during the photolysis of NO_2^-.

2. Experimental

2.1. Reagents

NDMA, DMA and sodium nitrite ($NaNO_2$) were obtained from Sigma–Aldrich, with purity higher than 99%. All chemicals used for making the solutions (buffer, eluents, etc.) were of reagent grade, and used without further purification. All stock solutions were prepared in distilled and deionized water (Barnstead NANO Pure, USA). Fifty millimolars aqueous stock solutions of NDMA, DMA and $NaNO_2$ were prepared and stored at room temperature, in the dark by covering with aluminum foil. The concentration of the NDMA stock solution was spectrophotometrically checked for variance prior to use.

2.2. Experimental apparatus and procedure

All experiments were performed in a 50 mL cylindrical Pyrex reactor, with an optical path length of 2 cm, with the solution exposed to UV supplied by four equivalent BLB lamps (Black Light Blue, Philips Co., USA.) emitting UV-A light of 300–400 nm (Fig. 1). The optical path length was chemically determined by photolysis kinetics of 2-nitrobenzaldehyde [11]. Most experiments were carried out open to atmosphere without gas purging (dissolved oxygen concentration ≈ 10 mg L^{-1}). For the experiments using gas purging, the upside of the reactor was sealed with a rubber septum, with O_2 or N_2 gas sparged through a needle-type diffuser. The solution pH was controlled to be constant (±0.2) during the reaction time by 2 mM phosphate buffer for pH 7 and 8.2, and by the continuous addition of an appropriate amount of 0.1 M NaOH solution for pH 9–11. The solution was vigorously mixed using a magnetic stirrer. The lamps were stabilized for about 30 min prior to their use for illumination. The incident photon flow (Einstein L^{-1} s^{-1}) was measured using ferrioxalate actinometry [12]. The photolytic production of Fe(II) was maintained at <10% of the initial amount of Fe(III) to insure complete light absorption by the ferrioxalate actinometer. An overall quantum yield of 1.2 was used in the calculation pertaining to the ferrioxalate photolysis reaction [13]. The measured incident photon intensity in this system was 1.4×10^{-5} Einstein L^{-1} s^{-1}.

The general experimental procedure was as follows: reaction solutions with specific concentrations of DMA and NO_2^-, or NDMA (for determining quantum yields in Table 1) were prepared by the addition of calculated aliquots of the stock solutions to distilled water; the pH was then adjusted to the desired value.

Table 1
Determined quantum yields for NDMA photolysis as a function of the pH under both O_2 and N_2 conditions: $[NDMA]_0 = 0.1$ mM, 310–370 nm

pH	O_2 condition	N_2 condition
7.0	0.314 ± 0.0021	0.318 ± 0.0141
8.2	0.309 ± 0.0105	0.317 ± 0.0108
9.0	0.206 ± 0.0124	0.043 ± 0.0037
10.0	0.166 ± 0.0152	0.025 ± 0.0014
11.0	0.184 ± 0.0149	0.015 ± 0.0006

The prepared solution was placed in the reactor, with a thermostat used to maintain the solution temperature at 25 ± 0.5 °C. The photolysis was initiated by exposing the reactor to UV irradiation. Samples were withdrawn at predetermined time intervals and rapidly analyzed. A set of triplicate photolysis experiments was carried out, with the mean and standard deviations values presented.

The quantum yield for NDMA photolysis due to the $n \rightarrow \pi^*$ transition (Φ) was determined by fitting the time-concentration profile of NDMA during the photolysis into Eq. (2)

$$\frac{d[NDMA]}{dt} = \sum I_\lambda \phi (1 - 10^{-\varepsilon_{\lambda,NDMA} L [NDMA]}) \quad (2)$$

where, I_λ is the incident photon flow at a given wavelength (Einstein s^{-1} L^{-1}), Φ the quantum yield for NDMA photolysis, $\varepsilon_{\lambda,NDMA}$ the molar absorption coefficient of NDMA at a given wavelength (λ) (M^{-1} cm^{-1}), and L is the optical path length (cm). I_λ values as a function of wavelength were calculated from the spectral distribution of the lamps, as measured by a spectrometer (Fig. 1), and the incident light intensity, as measured by ferrioxalate actinometry. The value of Φ determined in this study was an overall value for the approximate wavelength region 310–370 nm, as polychromatic irradiation was employed.

2.3. Analyses

The analyses of Fe(II) for ferrioxalate actinometry were carried out using the 1,10-phenanthroline method [14]. NDMA was analyzed by HPLC, using a SUPELCOGEL C−610H column (300 mm × 7.8 mm, 9 μm; Supelco Co., USA), employing UV detection at 230 nm. The mobile phase consisted of 0.1% H_3PO_4 solution, with a flow rate of 0.5 mL min^{-1}. The detection limit for NDMA was approximately 20 nM. The NDMA peak in the HPLC analysis was identified on a tandem mass spectrometer, with high mass resolution (FTQ Orbitrap, Thermo Electron Co., USA), employing positive electrospray ionization (ESI+). DMA and NO_2^- were analyzed using DX-120 ion chromatography (Dionex Co., USA) with a conductivity detector. DMA was analyzed with an IonPac CS14 cationic column (4 mm × 250 mm), using 10 mM methanesulfonic acid/0.3% acetonitrile solution as the eluent, with a flow rate of 1.0 mL min^{-1}. NO_2^- was analyzed with an IonPac AS14 anionic column (4 mm × 250 mm), using an 8.0 mM Na_2CO_3/1.0 mM $NaHCO_3$ solution as the eluent, with a flow rate of 1.0 mL min^{-1}. The detection limits for DMA and NO_2^- were approximately 1 μM. UV–vis spectra were taken on a Hewlett−Packard 8452 diode array spectrophotometer (USA). The emission spectrum of BLB lamp was measured using a Spectrapro-500 spectrometer (Acton Research Co., USA).

3. Results and discussion

3.1. Photochemical nitrosation of DMA to NDMA

Fig. 2 shows the time-dependent formation of NDMA during the photolysis of 1 mM NO_2^- in the presence of DMA. The photochemical nitrosation of DMA to NDMA during the photolysis

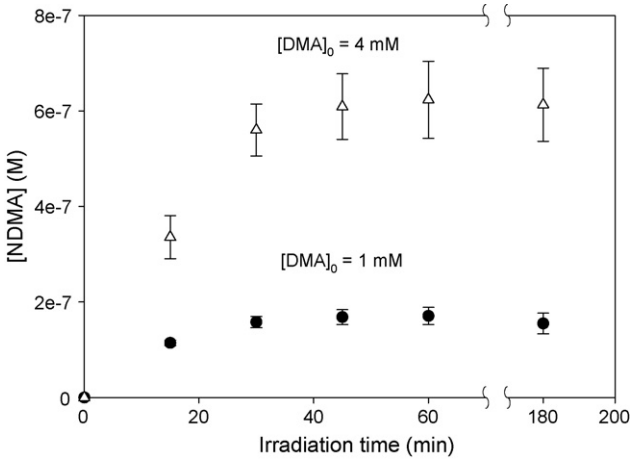

Fig. 2. NDMA formation in relation to the irradiation time: $[NO_2^-]_0 = 1$ mM and pH 7.0 (2 mM phosphate buffer).

of NO_2^- can be explained by reactions (3)–(8), as follows. The photolysis of NO_2^- is known to yield $NO^\bullet$ and $O^{\bullet-}$, with a quantum yield of 0.046 at 351 nm, as described in reaction (3) [7,15,16].

$$NO_2^- + h\nu \rightarrow NO^\bullet + O^{\bullet-}, \quad \phi = 0.046 \quad (3)$$

$O^{\bullet-}$ is protonated to form a hydroxyl radical ($^\bullet OH$) at pH < 11.9. $^\bullet OH$ either recombines with $NO^\bullet$ or reacts with NO_2^-, at a diffusion controlled rate, to produce $NO_2^\bullet$, which subsequently reacts with $NO^\bullet$ or another $NO_2^\bullet$ to form N_2O_3 or N_2O_4, respectively (reactions (4)–(6)).

$$^\bullet OH + NO_2^- \rightarrow NO_2^\bullet + OH^-, \quad k_3 = 1.0 \times 10^{10}\ M^{-1}\ s^{-1} \quad (4)$$

$$NO^\bullet + NO_2^\bullet \rightarrow N_2O_3, \quad k_4 = 1.1 \times 10^9\ M^{-1}\ s^{-1} \quad (5)$$

$$NO_2^\bullet + NO_2^\bullet \rightarrow N_2O_4, \quad k_5 = 4.5 \times 10^8\ M^{-1}\ s^{-1} \quad (6)$$

N_2O_3 and N_2O_4 are typical nitrosating agents of the type $NO^{\delta+}$–$Y^{\delta-}$ (where $Y = NO_2^-$ and NO_3^- for N_2O_3 and N_2O_4, respectively), and react with DMA to yield NDMA (reactions (7) and (8)).

$$N_2O_3 + DMA \rightarrow NDMA + NO_2^- + H^+ \quad (7)$$

$$N_2O_4 + DMA \rightarrow NDMA + NO_3^- + H^+ \quad (8)$$

In Fig. 2, the concentration of NDMA initially increased with irradiation time, but became constant as the rate of NDMA formation gradually decreased. This logarithmic increase in the concentration of NDMA with irradiation time was attributed to the enhanced photolysis of NDMA with increasing concentration. No significant reductions in the concentrations of NO_2^- and DMA were observed with increasing reaction time (data not shown). The NDMA concentrations after 60 min UV irradiation were 1.7×10^{-7} and 6.2×10^{-7} M, with 1 and 4 mM DMA, respectively; indicating the photochemical yields of NDMA from DMA are only 0.015–0.017%. These values were much lower than those previously reported [8], which showed up to a 35% conversion of DMA to NDMA in the presence of 5 mM

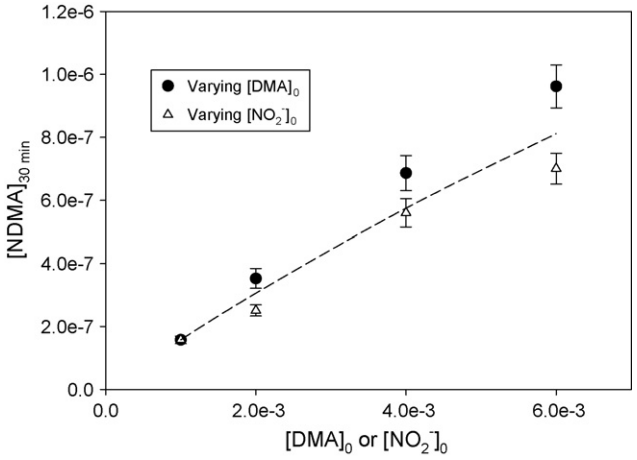

Fig. 3. NDMA formation (after 30 min irradiation) as a function of $[DMA]_0$ ($[NO_2^-]_0 = 1$ mM) or $[NO_2^-]_0$ ($[DMA]_0 = 1$ mM): pH 7.0 (2 mM phosphate buffer). The dashed line represents the model prediction by varying the $[NO_2^-]_0$.

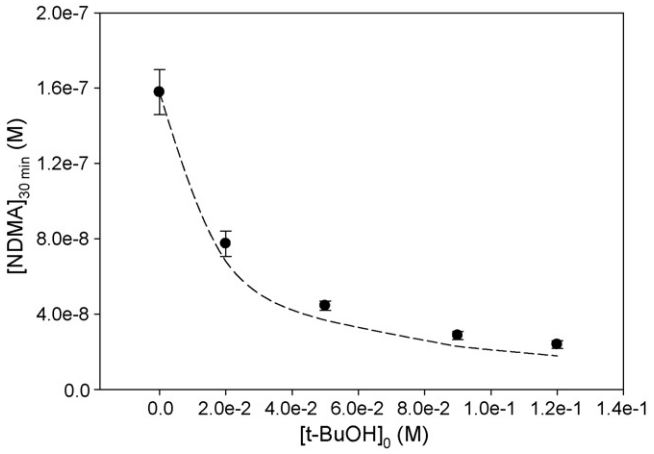

Fig. 4. Effects of $^{\bullet}OH$ scavenger (*t*-BuOH) on the formation of NDMA (after 30 min irradiation): $[NO_2^-]_0 = 1$ mM, $[DMA]_0 = 1$ mM and pH 7.0 (2 mM phosphate buffer). The dashed line epresents the model prediction.

NO_2^- ($[DMA]_0$:$[NO_2^-]_0 = 1{:}1$) after 15 h of UV irradiation from a medium pressure Hg lamp; we have no explanation for this discrepancy. However, a simple comparative calculation of the photolysis rates of NO_2^- and NDMA shows that the result in the previous study is unreasonable. The molar absorption coefficients of NDMA, and their photolytic quantum yields ($\varepsilon = 40.6\ M^{-1}\ cm^{-1}$, averaged value in 300–400 nm; $\phi = 0.31$ (Table 1)) were approximately 2.9- and 6.7-fold higher than those of NO_2^- ($\varepsilon = 14.0\ M^{-1}\ cm^{-1}$, averaged value in 300–400 nm (Fig. 1); $\phi = 0.046$ at 351 nm [16]), respectively. Hence, the rate of NDMA photolysis may be (2.9×6.7) 19.4-fold higher than that of NO_2^-, indicating the steady state concentration of NDMA cannot exceed 5.2% ($1/19.4 \times 100$) of $[NO_2^-]_0$. In fact, the concentration of NDMA should be much lower, depending on the yield of nitrosating agents produced during the photolysis of NO_2^- that is able to react with DMA.

3.2. Effects of concentrations of NO_2^- and DMA

The NDMA concentration after 30 min of UV irradiation ($[NDMA]_{30\ min}$), when varying the initial concentrations of DMA and NO_2^- ($[DMA]_0$ and $[NO_2^-]_0$) was measured. As shown in Fig. 3, $[NDMA]_{30\ min}$ increased with increasing $[DMA]_0$ or $[NO_2^-]_0$. First, the enhancement of NDMA formation with $[NO_2^-]_0$ is explained by the photon flow absorbed by NO_2^- (I_{a,NO_2^-}).

$$I_{a,NO_2^-} = I_0(1 - 10^{-\varepsilon_{NO_2^-} L[NO_2^-]}) \quad (9)$$

where, I_0 is the incident photon flow (Einstein $s^{-1}\ L^{-1}$), $\varepsilon_{NO_2^-}$ the molar absorption coefficient of NO_2^- ($14.0\ M^{-1}\ cm^{-1}$, averaged value in 300–400 nm) and L is the optical path length of the reactor (2 cm). The formation of NDMA is proportional to I_{a,NO_2^-} and; thereby, $[NDMA]_{30\ min}$ as a function of $[NO_2^-]_0$ can be simply modeled from the value at $[NO_2^-]_0 = 1$ mM using Eq. (10). Where, $[NDMA]_{30\ min,Ini}$ is the $[NDMA]_{30\ min}$ value at $[NO_2^-]_0 = 1$ mM and $I_{a,NO_2^-,Ini}$ is the I_{a,NO_2^-} value at $[NO_2^-]_0 = 1$ mM. The dashed line in Fig. 3 represents the model calculation.

$$[NDMA]_{30\ min} = \frac{I_{a,NO_2^-}}{I_{a,NO_2^-,Ini}} \times [NDMA]_{30\ min,Ini} \quad (10)$$

Second, the dependence of NDMA formation on $[DMA]_0$ is explained by the competition between the reactions of the nitrosating agents with DMA (reactions (7) and (8)) and their subsequent hydrolyses. The nitrosating agents (N_2O_3 and N_2O_4) produced during NO_2^- photolysis are unstable and known to be readily hydrolyzed to NO_2^- and NO_3^- [17,18] unless they react with DMA.

3.3. Effects of a $^{\bullet}OH$ scavenger

As described in reactions (4)–(6), $^{\bullet}OH$ plays an important role in producing nitrosating agents during the photolysis of NO_2^- by its oxidation to yield $NO_2^{\bullet}$. In order to verify this role of $^{\bullet}OH$ in the photochemical formation of NDMA, *t*-BuOH was employed as a $^{\bullet}OH$ scavenger. Fig. 4 shows the $[NDMA]_{30\ min}$ as a function of the initial *t*-BuOH concentration added ($[t\text{-BuOH}]_0$). $[NDMA]_{30\ min}$ was found to exponentially decrease with increasing $[t\text{-BuOH}]_0$. When 0.12 M *t*-BuOH was added to the solution, the $[NDMA]_{30\ min}$ was reduced by 85%, from 1.6×10^{-7} to 2.4×10^{-8} M. The $[NDMA]_{30\ min}$ as a function of $[t\text{-BuOH}]_0$ was modeled from $[t\text{-BuOH}]_0 = 0$, using a simple equation for the competition kinetics of reactions (4) and (11) (Eq. (12)), which is presented in Fig. 4 (dashed line). The model calculation was in a good agreement with the experimental result [19].

$$^{\bullet}OH + t\text{-BuOH} \rightarrow k_{15} = 6.6 \times 10^8\ M^{-1}\ s^{-1} \quad (11)$$

$$[NDMA]_{30\ min} = \frac{k_4[NO_2^-]_0}{k_4[NO_2^-]_0 + k_{15}[t\text{-BuOH}]_0} \times [NDMA]_{30\ min,Ini} \quad (12)$$

where, $[NDMA]_{30\ min,Ini}$ is the $[NDMA]_{30\ min}$ value at $[t\text{-BuOH}]_0 = 0$.

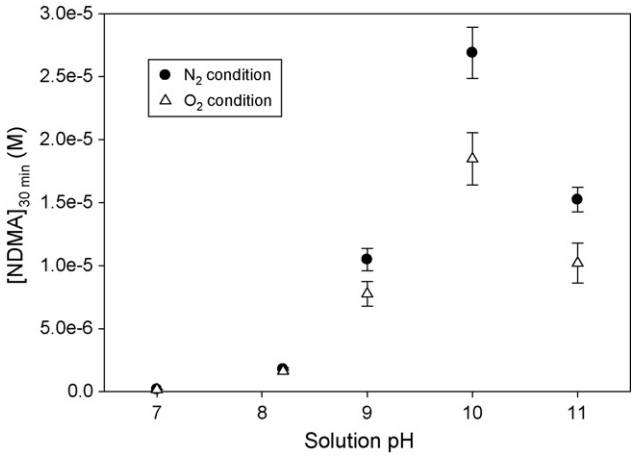

Fig. 5. Measured (symbols) and predicted (dashed lines) formations of NDMA (after 30 min irradiation) as a function of the pH under both O_2 and N_2 conditions: $[NO_2^-]_0$ = 1 mM, $[DMA]_0$ = 1 mM, and [phosphate ion]$_0$ = 2 mM.

3.4. pH dependence

Fig. 5 shows the pH dependence of $[NDMA]_{30\ min}$ in the pH range 7–11 under both O_2 and N_2 conditions. The formation of NDMA was strongly pH dependent, with a maximum around pH 10 under both O_2 and N_2 conditions. The maximum $[NDMA]_{30\ min}$ was found to be higher under N_2 than O_2 conditions. The $[NDMA]_{30\ min}$ increased by more than 100-fold, from 1.6×10^{-7} to 1.8×10^{-5} M (NDMA yield = 1.8%), under O_2 conditions, and by 150-fold, from 1.7×10^{-7} to 2.7×10^{-5} M (NDMA yield = 2.7%), under N_2 conditions, as the solution pH increased from 7 to 10. The $[NDMA]_{30\ min}$ decreased at pH 11 under both O_2 and N_2 conditions. The pH dependent $[NDMA]_{30\ min}$ values under air conditions, without gas sparging, were almost the same as those obtained under O_2 conditions.

The pH dependence of the formation of NDMA can mainly be explained by the dual role of DMA as a nucleophile and a hydroxyl radical ($^{\bullet}OH$) scavenger. First, the reactions of nitrosating agents with DMA (reactions (7) and (8)) are known to be nucleophilic substitution (S_N2) of anion moiety (–Y) in the nitrosating agent ($NO^{\delta+}$–$Y^{\delta-}$) with DMA, which acts as a nucleophile [6]. The protonated form of DMA (DMA–H^+) cannot serve as an effective nucleophile. Hence, the rates of the reactions shown in (7) and (8) are proportional to the concentration of deprotonated DMA ([DMA]), which increases with increasing solution pH up to 10.7 (pK_a of DMA).

Conversely, the deprotonated form of DMA can be a strong $^{\bullet}OH$ scavenger. As shown in Fig. 4, the $^{\bullet}OH$ scavenger inhibits the production of nitrosating agents by competing for $^{\bullet}OH$ and NO_2^-. In general, the deprotonated amine is a strong electron donor, with a rate constant for its reaction with $^{\bullet}OH$ approximately two orders of magnitude higher than that of the protonated form. Although the rate constant for the reaction of deprotonated DMA with $^{\bullet}OH$ has not been reported, it is assumed the value will be within the range 10^9 to 10^{10} M^{-1} s^{-1}, based on the values of methylamine and trimethylamine [20]. In addition, less stability of nitrosating agents in higher pH region can also influence the decrease of $[NDMA]_{30\ min}$ at pH 11. According to a previous study [21], the rate constant for the hydrolysis of N_2O_3 was found to linearly increase with $[OH^-]$.

A higher $[NDMA]_{30\ min}$ under N_2 condition may result from the lower quantum yields for the photolysis of NDMA, which occurs simultaneously with its formation. Table 1 summarizes the quantum yields for the photolysis of NDMA due to the $n \rightarrow \pi^*$ transition as a function of pH under both O_2 and N_2 conditions. The quantum yields were constant, at around 0.31, in the pH region 7–8.2 under both N_2 and O_2 conditions. However, under alkaline conditions, in the pH region 9–11, the quantum yields under N_2 conditions were obviously lower than those under O_2 conditions, after a drastic drop at around pH 9. The photolytic behaviors of NDMA were solution pH and dissolved oxygen dependent, and similar to those observed in the photolysis of NDMA via the $\pi \rightarrow \pi^*$ transition, which may originate from the speciation of photo-excited NDMA and its photooxidation mechanism [9,10].

3.5. Effects of anions

Fig. 6 shows the $[NDMA]_{30\ min}$ as a function of the phosphate ion concentration ($[PO_4^{3-}]_0$) at pH 7 and 8.2, which indicates that the phosphate ion employed in the buffer solution significantly inhibits the photochemical formation of NDMA. When the $[PO_4^{3-}]_0$ was increased from 2 to 8 mM, the $[NDMA]_{30\ min}$ was reduced by 42 and 67, from 5.6×10^{-7} to 3.2×10^{-7} M, and from 4.7×10^{-6} to 1.5×10^{-6} M at pH 7 and 8.2, respectively. The greater reduction in the $[NDMA]_{30\ min}$ at pH 8.2 indicates that HPO_4^{2-} is a stronger inhibitor than $H_2PO_4^-$ (pK_a of $H_2PO_4^-$ = 7.2).

The phosphate ion cannot serve as a $^{\bullet}OH$ scavenger to compete with NO_2^- since the rate constants for the reactions of $H_2PO_4^-$ and HPO_4^{2-} are $\sim 2 \times 10^4$ and 1.5×10^5 M^{-1} s^{-1}, respectively [19]. The inhibitory effect of the phosphate ion on the formation of NDMA can be explained as follows. According to a previous study [22], one nitrosating agent can be converted to another by its reaction with anions. In the presence of phosphate ions, the N_2O_3 or N_2O_4 produced during NO_2^- photolysis may react with phosphate ion to form another nitrosating agent

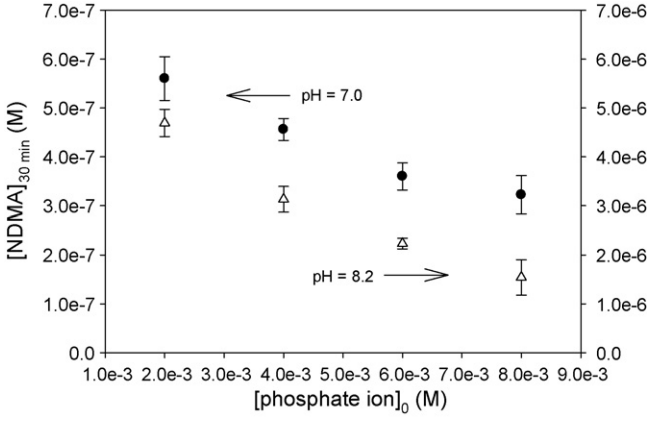

Fig. 6. Effects of phosphate ions on the formation of NDMA (after 30 min irradiation): $[NO_2^-]_0$ = 1 mM and $[DMA]_0$ = 4 mM.

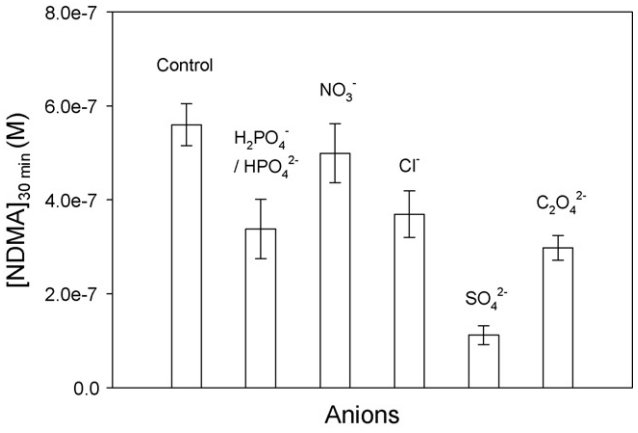

Fig. 7. Effects of anions on the formation of NDMA (after 30 min irradiation): $[NO_2^-]_0 = 1$ mM, $[DMA]_0 = 4$ mM, $[anion]_0 = 5$ mM, and pH 7.0 (2 mM phosphate buffer).

of H_2PO_4–NO, as described in reaction (13).

$$N_2O_3\ (\text{or}\ N_2O_4) + HPO_4^{2-}/H_2PO_4^- \rightarrow H_2PO_4\text{–NO}\ (H^+) + NO_2^-\ (\text{or}\ NO_3^-) \quad (13)$$

If H_2PO_4–NO is less reactive toward DMA, or more readily hydrolyzed than the parent nitrosating agents, the formation of NDMA can be inhibited.

In order to investigate this effect of anions, the $[NDMA]_{30\ min}$ was measured in buffered solutions (2 mM phosphate buffer) containing a comparable amount of various anions (5 mM), such as HPO_4^{2-} ($H_2PO_4^-$), NO_3^-, Cl^-, SO_4^{2-} and $C_2O_4^{2-}$ (Fig. 7). Interestingly, the inhibitory effect on the formation of NDMA was observed with all the anions, with the high-valent anions (SO_4^{2-} and $C_2O_4^{2-}$) tending to serve as stronger inhibitors. None of the anions used in Fig. 7, with the exception of Cl^-, act as $^\bullet$OH scavengers [19], indicating these anions inhibit the formation of NDMA by transforming N_2O_3 or N_2O_4 into less effective forms.

On the other hand, Cl^- is a strong $^\bullet$OH scavenger, with a rate constant of $4.3 \times 10^9\ M^{-1}\ s^{-1}$ for its reaction with $^\bullet$OH, indicating that inhibitory effect of Cl^- mainly results from its role as a $^\bullet$OH scavenger. A simple calculation, using the competition kinetics of Cl^- and NO_2^- for $^\bullet$OH, predicts that 5 mM Cl^- used as a $^\bullet$OH scavenger reduces the $[NDMA]_{30\ min}$ by 68%, from 6.5×10^{-7} to 1.8×10^{-7} M. On the contrary, in Fig. 7, a lower-than-expected effect of 5 mM Cl^- ($[NDMA]_{30\ min} = 3.7 \times 10^{-7}$ M) was observed. Two possible explanations can be suggested for this observation. First, $Cl^\bullet$ produced from the reaction of Cl^- with $^\bullet$OH can also oxidize NO_2^- into $NO_2^\bullet$ as $^\bullet$OH does. Second, the nitrosating agent formed by the reaction of N_2O_3 or N_2O_4 with Cl^- (NO–Cl) can be more reactive than the parent nitrosating agents (N_2O_3 or N_2O_4). Several previous studies have reported higher nitrosating activities of NO–Cl than N_2O_3 during the nitrosation of morpholine [22,23].

4. Conclusion

In this study, the UV-A induced photochemical formation of NDMA in the presence of DMA and NO_2^-, was investigated by varying several experimental parameters, such as the concentrations of DMA and NO_2^-, solution pH, dissolved oxygen and the presence of a hydroxyl radical ($^\bullet$OH) scavenger or anions in aqueous solution. The principle results obtained can be summarized as follows: NDMA was formed from DMA during the photolysis of NO_2^- under neutral and alkaline pH conditions, with yields of 0.015% (pH 7)–2.7% (pH 10, N_2 condition), which are much lower than those reported in a previous study. The formation of NDMA was enhanced by increasing the concentrations of DMA and NO_2^-. The addition of a $^\bullet$OH scavenger significantly inhibited the formation of NDMA by suppressing the production of $NO_2^\bullet$, which is a precursor of the nitrosating agents formed during the photolysis of NO_2^-. The maximal formation of NDMA, at around pH 10, was effectively explained by the dual role of the deprotonated DMA as a nucleophile and a $^\bullet$OH scavenger. Lower quantum yields for the photolysis of NDMA in the absence of oxygen yielded a relatively higher formation of NDMA under N_2 condition. Various anions inhibited the formation of NDMA, possibly due to degradation of the nitrosating agents. However, the inhibitory effect of Cl^- was mainly due to its role as a $^\bullet$OH scavenger. On the other hand, with the nitrosation yields of 0.015–0.18% (pH 7–8.2) obtained in this study, the concentration of NDMA formed by the NO_2^- photolysis in natural waters is predicted to be $<10^{-9}$ M since NO_2^- and DMA concentrations in those waters are usually $<10^{-6}$ M. Dissolved organic matters serving as $^\bullet$OH scavengers and anions in natural waters can lead to even lower yields.

Acknowledgement

This research was partially supported by the Brain Korea 21 Program of the Ministry of Education.

References

[1] S.D. Richardson, Trends Anal. Chem. 22 (2003) 666–684.
[2] W.A. Mitch, J.O. Sharp, R.R. Trussell, R.L. Valentine, L. Alvarenz-Cohen, D.L. Sedlak, Environ. Eng. Sci. 20 (2003) 389–404.
[3] W.A. Mitch, D.L. Sedlak, Environ. Sci. Technol. 36 (2002) 588–595.
[4] J. Choi, R.L. Valentine, Wat. Res. 36 (2002) 817–824.
[5] I. Najm, R.R. Trussell, J. AWWA Feb. (2001) 92–99.
[6] S. Patai, The Chemistry of Amino, Nitroso and Nitro Compounds and their Derivatives, Interscience, John Wiley and Sons, London, New York, 1982.
[7] J. Mack, J.R. Bolton, J. Photochem. Photobiol. A: Chem. 128 (1999) 1–13.
[8] T. Ohta, J. Suzuki, Y. Iwano, S. Suzuki, Chemosphere 11 (1982) 797–801.
[9] C. Lee, W. Choi, Y.G. Kim, J. Yoon, Environ. Sci. Technol. 39 (2005) 2101–2106.
[10] C. Lee, W. Choi, J. Yoon, Environ. Sci. Technol. 39 (2005) 9702–9709.
[11] C. Lee, J. Yoon, Chemosphere 56 (2004) 923–934.
[12] C.G. Hatchard, C.A. Parker, Proc. Roy. Soc. Lon. A 235 (1956) 518–536.
[13] V. Balzani, V. Carassitti, Photochemistry of Coordination Compounds, Academic Press, London, New York, 1970.
[14] H. Tamura, K. Goto, T. Yotsuyanagi, M. Nagayama, Talanta 21 (1974) 314–318.
[15] O.C. Zafirou, M.B. True, Mar. Chem. 8 (1979) 9–32.
[16] R. Zellner, M. Exner, H. Herrman, J. Atmos. Chem. 10 (1990) 411–425.

[17] P. Bilski, C.F. Chignell, J. Szychlinski, A. Borkowski, E. Oleksy, K. Reszka, J. Am. Chem. Soc. 114 (1992) 549–556.
[18] M.C. Gonzalez, A.M. Braun, J. Photochem. Photobiol. A: Chem. 93 (1996) 7–19.
[19] G.V. Buxton, C.L. Greenstock, W.P. Helman, A.B. Ross, J. Phys. Chem. Ref. Data 17 (1988) 513–886.
[20] S. Kim, W. Choi, Environ. Sci. Technol. 36 (2002) 2019–2025.
[21] A. Treinin, E. Hayon, J. Am. Chem. Soc. 92 (1970) 5821–5828.
[22] R.S. Lewis, S.R. Tannenbaum, W.M. Deen, J. Am. Chem. Soc. 117 (1995) 3933–3939.
[23] T.-Y. Fan, S.R. Tannenbaum, J. Agric. Food Chem. 21 (1973) 237–240.